Synthesis and Structural Characterization of Cr_2O_3 Nanoparticles Prepared by Using $Cr(NO_3)_3.9H_2O$ and Triethanolamine Under Microwave Irradiation

Tagreed. M. Al-Saadi

Department of Physics, College of Education for Pure Science Ibn-Al-Haithm , University of Baghdad, Baghdad, Iraq

Noor A. Hameed

Department of Physics, College of Science, University of Diyala, Diyala, Iraq

Abstract

In this study, Chromium oxide nanoparticles (Cr_2O_3-NPs) was prepared by sol-gel method, using $Cr(NO_3)_3.9H_2O$ as a Precursor material, triethanolamine (TEA) as a template and water as green solvent under microwave irradiation . X- ray diffraction (XRD), Scanning electron microscopy (SEM), Rietveld refinement and Fourier Transform Infrared spectroscopy (FTIR) were employed to characterize the average crystallite size, crystalline structure, morphology, unit cell parameters and chemical groups of the annealed powder. From XRD data and Dicvol 91 software analysis, the crystal system was found to be rhombohedral structure for samples. The average crystallite size is calculated by using Debye-Scherrer formula, crystallites size and strain are calculated by using Williamson-Hall formula. The effect of particle size on the crystal lattice distortion ratio, specific surface area, dislocation density and number of unit cell was discussed. A good agreement is between XRD data and FIR data. The qualitative phase analysis is performed by Rietveld analysis using "Fullprof" program of Cr_2O_3-NPs.

Keywords: Cr_2O_3, Nanoparticles, Sol – Gel , Structural Properties, Rietveld refinement.

1.   Introduction

Nano size materials exhibit unique electronic, magnetic, optical, catalytic and medicinal properties as compared with the traditional and commercial bulk materials. It is due to its quantum size effect, large surface to volume ratio [1].Chromium (III) oxide belongs to rhombohedral crystal system and is of great interest due to its easiness of preparation and it has a wide range of applications such as heterogeneous catalyst [1], pigments to reflect infrared radiation [2], solar energy application [3], high temperature resistant materials because of its high melting temperature ($\approx 2300°C$) [3,4], liquid crystal displays [5], wear resistance [6] and coating material [7]. Different methods are available to prepare Cr_2O_3-NPs such as sol-gel technique [8], sonochemical method [9], precipitation-gelation [10], mechanochemical process [11], microwave plasma [12] and gas condensation [13], etc.

In the present study, we have synthesized (Cr_2O_3-NPs) under microwave irradiation using TEA as template and water as a green solvent.

2- Experimental Part

2-1 Synthesis

All chemicals and reagents were of synthetic grade and used without further purification. In a typical procedure, 50 ml of $Cr(NO_3)_3.9H_2O$ (0.2M) (99.5%, Fluka) aqueous solution was mixed with appropriate amount of triethanolamine ($C_6H_{15}NO_3$) (99.5%, Fluka) as template (20 and 30 mmol). After stirring for 1 hour, the mixture was placed under microwave irradiation for 3 min. The green solid product was centrifuged and dried in air at room temperature . Six samples were prepared , first three by adding 20 mmol of (TEA) and second there by adding 30 mmol (TEA) , then annealed at 500 °C and 600°C for 2 h ,the details of these samples are shown in table (1).

Table 1. Concentration of triethanolamine (TEA) at various annealing temperature of Cr_2O_3-NPs

(TEA)	Annealing temperature	Sample
20 mmol	As prepared	S1
	Annealed at 500˚C	S2
	Annealed at 600˚C	S3
30 mmol	As prepared	S4
	Annealed at 500˚C	S5
	Annealed at 600˚C	S6

2-2 Characterization

The crystalline structure of the prepared powders was determined by X-ray diffraction (Shimadzu XRD-6000) with Cu $K\alpha_1$ radiation. The average crystallite size (D) of each powder was estimated from the Scherrer formula and Williamson-Hall formula.

The powder morphology was observed using a (VEGA\\Easy Probe) scanning electron microscope. Fourier transformation infrared spectroscopy analysis of annealed powders was carried out in Shimadzu equipment (IRAffinity-1 FTIR Spectrophotometer) for studying the chemical groups of the annealed powder. Rietveld analysis was carried out to calculate unit cell parameters.

3- Results and Discussion

3-1 XRD measurement

The XRD pattern of all the samples ,Cr_2O_3 nanoparticles (NPs)as prepared , annealed at 500°C and 600°C by using (20 and 30) mmol of triethanolamine (TEA) are shown in figure (1). They were compared with JCPDS file No.38-1479 and no crystalline impurities were detected. The observed diffraction peaks correspond to the rhombhedral crystalline Cr_2O_3 (Eskolaite) with space groupe (R $\bar{3}$ c). The results of diffraction angle (2θ), full width at half maximum (FWHM) β, spacing between crystal planes (d) for three strongest peaks are shown in table (2).

3-2 Crystallite Size Calculation

The average crystallite size for synthesized Cr_2O_3 was determined by Debye-Scherrer's equation [14-17]:
$$D = K\lambda / \beta_D \cos\Theta \quad \ldots\ldots(1)$$
where D: crystallite size, K: constant, λ: wavelength of Cu kα radiation and β_D: is the broadening due to small crystallite size.
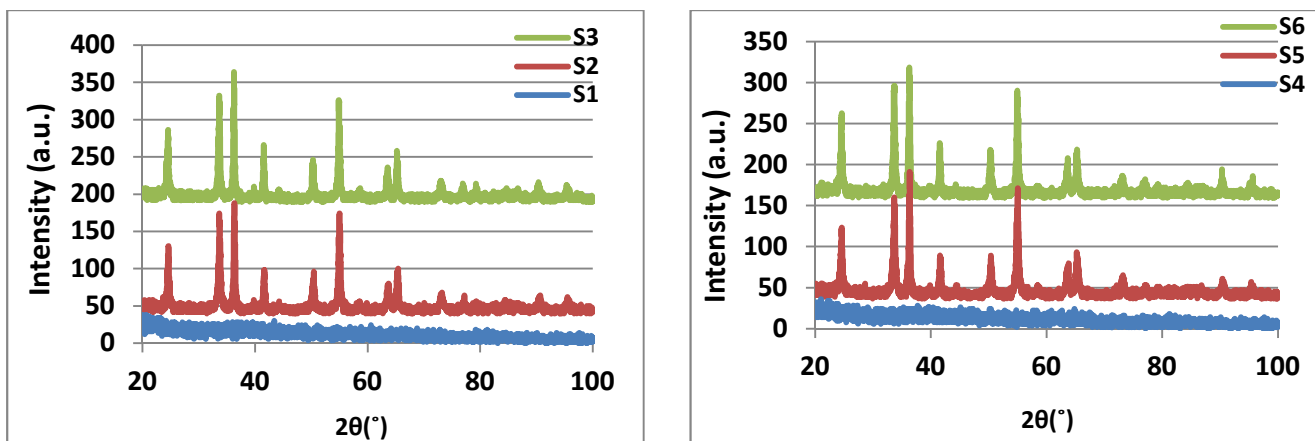
Figure 1. XRD patterns of Cr_2O_3-NPs.

The crystallite size and lattice strain induced in powders arising from defects like dislocation, twinning, imperfection and distortion was determined by Williamson-Hall equation [18]:
$$\beta_{hkl} \cos\Theta = (K\lambda / D) + (4\varepsilon \sin\Theta) \quad \ldots\ldots(2)$$
W-H plot is shown in figure (2). It is plotted with sinΘ on the x-axis and $\beta_{hkl} \cos\Theta$ on the y-axis (β_{hkl} in radian). Table (3) shows strain and crystallite size according to W-H and crystallite size according to Debye-Scherrer for Cr_2O_3 nanoparticles.

Table 2. XRD data of Cr_2O_3-NPs

Sample	$2\theta(°)$	$d(Å)$	$\beta(°)$	I/I_1
S1	22.3674	3.97153	0.048	100
	29.5529	3.02021	0.078	100
	30.4793	2.93049	0.073	100
S2	36.335	2.470	0.304	100
	54.978	1.668	0.395	91
	33.706	2.656	0.345	89
S3	36.264	2.475	0.304	100
	54.901	671	0.310	95
	33.623	2.663	0.382	88
S4	35.082	2.555	0.070	100
	35.697	2.513	0.120	100
	39.7390	2.26640	0.110	100
S5	36.318	2.471	0.329	100
	54.971	1.669	0.424	87
	33.675	2.659	0.400	76
S6	36.296	2.473	0.295	100
	54.942	1.670	0.313	92
	33.667	2.660	0.344	91
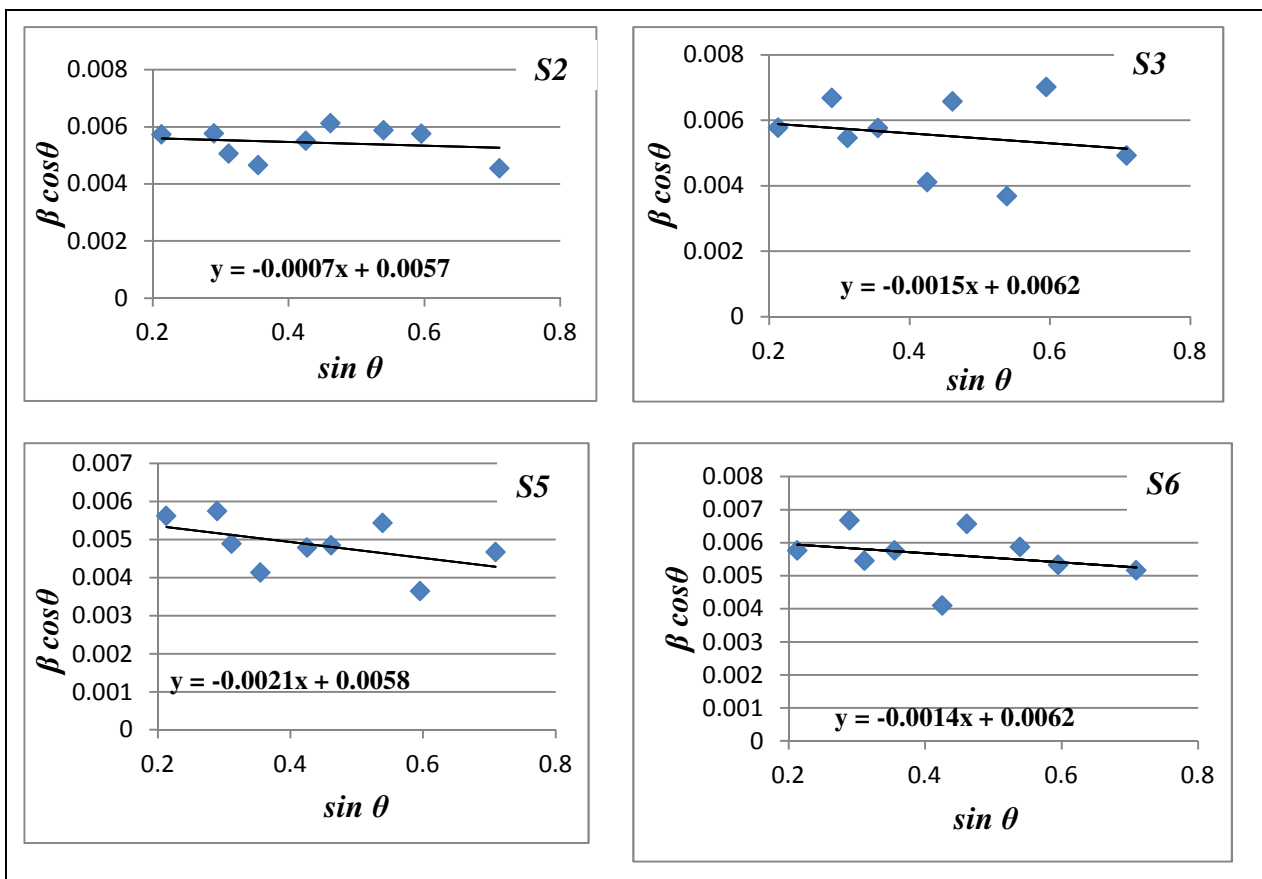
Figure 2. Williamson Hall plot of Cr_2O_3-NPs

Table 3**.** Strain and crystallite size according to W- H and crystallite size according
to D-S of Cr_2O_3-NPs

Sample	D (W-H)nm	ε (W-H)*10^{-4}	D (D-S) nm
S2	25.7	-1.75	23.1
S3	26.5	-3.75	24.3
S5	27.9	-5.25	22.3
S6	29.2	-3.5	23.9

From table (3) it shows that the average crystallite size increases with the increase of annealing temperature and concentration of (TEA) because of decreases in the density of nucleation centers, thus a smaller number of centers starts to grow, resulting in large crystallites. Generally the average crystallite size depends on the annealing temperature[19,20]. The difference between crystallite size according to W-H and crystallite size according to Debye-Scherrer occurs because W-H method takes into account the lattice strain of crystallite arising from defects like dislocation, twinning, imperfection and distortion. A negative value for the strain is due to lattice shrinkage [21].

The crystal lattice distortion ratio of Cr_2O_3-NPs at different annealing temperatures and concentrations of (TEA) are calculated by using equation (3)[26]:

$$\beta_{hkl}{}^2 \cos^2\Theta = (4\lambda^2/\pi^2 D^2) + 32\langle\varepsilon^2\rangle \sin^2\Theta \quad \ldots\ldots(3)$$

From equations (1and 3), it can be deduced the lattice distortion ratio used in the form of equation (4):

$$\sqrt{\langle\varepsilon^2\rangle} = \frac{1}{D}\frac{1}{sin\theta}\frac{\pi}{\lambda}\sqrt{\frac{\pi^2 k^2 - 4}{32}} \qquad \ldots\ldots(4)$$

Where $<\varepsilon^2>^{1/2}$ is the crystal lattice distortion ratio, it is shown in table (4) for S2, S3, S5 and S6 of Cr_2O_3-NPs.

Table 4. Crystal lattice distortion ratio of Cr_2O_3-NPs

Sample	D (W-H) nm	lattice distortion ratio
S2	25.7	0.0268
S3	26.5	0.0230
S5	27.9	0.0251
S6	29.2	0.237

The crystal lattice distortion ratio decreases with the increase of the average crystallite size and annealing temperature

3-3 Specific Surface Area (SSA)
SSA is the area per unit mass, it is a factor to determine bulk rates of such reactions (unit m^2/g) [22]. It is very important in the nanoparticles because their large surface to volume ratio with a decrease in particle size[23]. SSA is used in materials to determine their types and properties and is also used in case of reactions on surfaces, heterogeneous catalysis and adsorption[24].
Mathematically, SSA can be determined by using equation (5)[25]. Specific surface area of Cr_2O_3 nanoparticles is shown in table (5).

$$SSA = 6 * 10^3 / D_p \rho \qquad \ldots\ldots(5)$$

Where ρ is the density of Cr_2O_3 (5.22 g.cm^{-3}).

From table (5); it is clear that SSA increases when the particle size and annealing temperature decreases because of the degree of agglomeration by the effect of annealing occurring in the material.

Table 5. Specific surface area of Cr_2O_3-NPs

Sample	D (W-H) nm	SSA ($m^2. g^{-1}$)	D (D-S) nm	SSA ($m^2. g^{-1}$)
S2	25.7	44.7	23.1	49.7
S3	26.5	43.3	24.3	47.3
S5	27.9	41.1	22.3	51.5
S6	29.2	39.2	23.9	48.1

3-4 Rietveld Refinment

Rietveld refinement is a technique used to solve a structure crystalline materials from the powder diffraction data . The results powder diffraction from X-ray are characterized by reflections as a peak , intensity at certain position. The position, height and width for peak can be used to determine the material's structure. The Rietveld method uses a least squares to reduce the difference between the calculated and observed patterns , if the value of χ^2 is close to 1, that indicates the appropriate quality between observation and calculated data [27–29]. Rietveld refinements of Cr_2O_3-NPs for S2, S3, S5 and S6 are shown in figure (3) and the results of indexing and refinement are shown in table (6).
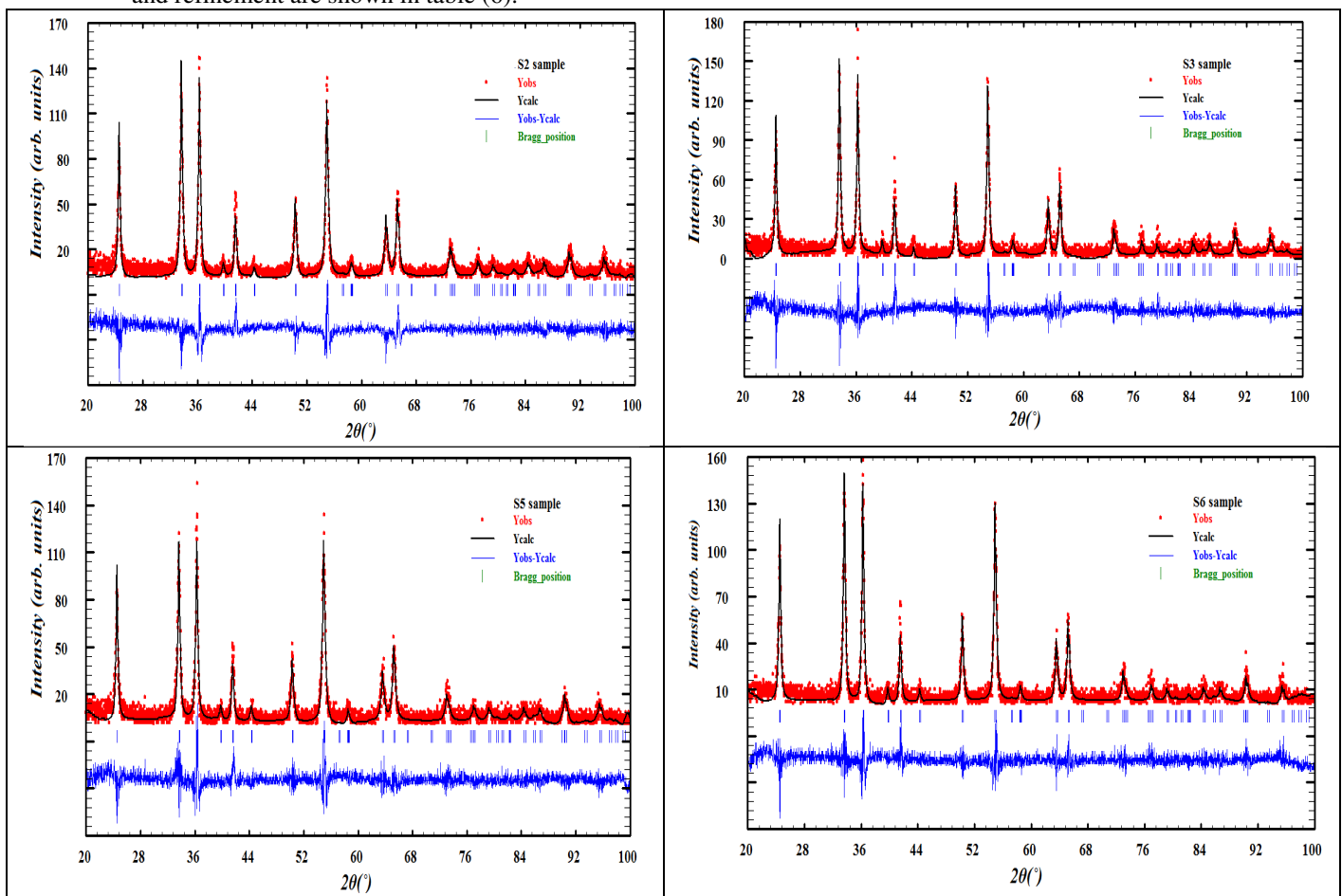
Figure 3. Rietveld refinements of Cr_2O_3-NPs for S2, S3, S5 and S6 samples.
The experimental points are plotted as dots (.) and theoretical data are shown as solid line. The difference between theoretical and experimental data is shown in the bottom line of each figure. The vertical lines represent the Bragg's allowed peaks.

143

Table 6. The results of indexing and refinement for Cr2O3-NPs.

Sample	Unit cell parameters (Å)		Crystal System	Space group	Angles (°)		Atomic Position				χ^2
	a=b	c			α= β	γ	atom	x	y	z	
S2	4.948	13.582	Rhom.	R $\bar{3}$ c	90	120	Cr	0.0	0.0	0.3478	1.93
							O	0.3047	0.0	0.25	
S3	4.951	13.593	Rhom.	R $\bar{3}$ c	90	120	Cr	0.0	0.0	0.3472	1.80
							O	0.3077	0.0	0.25	
S5	4.949	13.580	Rhom.	R $\bar{3}$ c	90	120	Cr	0.0	0.0	0.3447	1.53
							O	0.3134	0.0	0.25	
S6	4.952	13.589	Rhom.	R $\bar{3}$ c	90	120	Cr	0.0	0.0	0.3469	1.57
							O	0.3043	0.0	0.25	

From figure (3) it is noticed that peak width of decreases with the increaseg of the annealing temperature are due to growth of crystallite and construction to larger clusters.

3-5 Dislocation Density

Dislocation density (δ) is the length of the dislocations present per unit area (lines/m^2). It is an important property for material. Many of the properties of materials are affected by dislocation, it is a crystallographic defect, or irregularity, within a crystal structure[30]. Dislocation density depends on the materials microstructure. The dislocation density is measured by direct methods, such as transmission electron microscopy (TEM) techniques, and by indirect methods, such as X-ray diffraction (XRD) or neutron techniques [31, 32]. The dislocation density (δ) in the samples is calculated by using equation (6)[9, 26].

$$\delta = \frac{15\,\beta\,Cos\,\theta}{4\,a\,D} \quad ......(6)$$

Where, δ: dislocation density and α: lattice constant (nm).
And also can be calculated from equation (7).

$$\delta = \frac{1}{D^2} \quad ....(7)$$

The number of unit cell is calculated from equation (8).
n = π (4/3) . (D/2)^3 . (1/V) ......(8)

where n: the number of unit cell and V: is the cell volume.

The number of unit cell Vs dislocation density and versus particle size of Cr$_2$O$_3$-NPs for S2, S3, S5 and S6 are shown in figure (4 and 5) respectively.

From figures (4 and 5); it shows that dislocation density decreases and the number of unit cells increases with the increase in particle size and calcination temperatures that leads to increase the crystal growth and decrease the defects in crystallites, that means the crystals with larger dislocation density were harder [34].
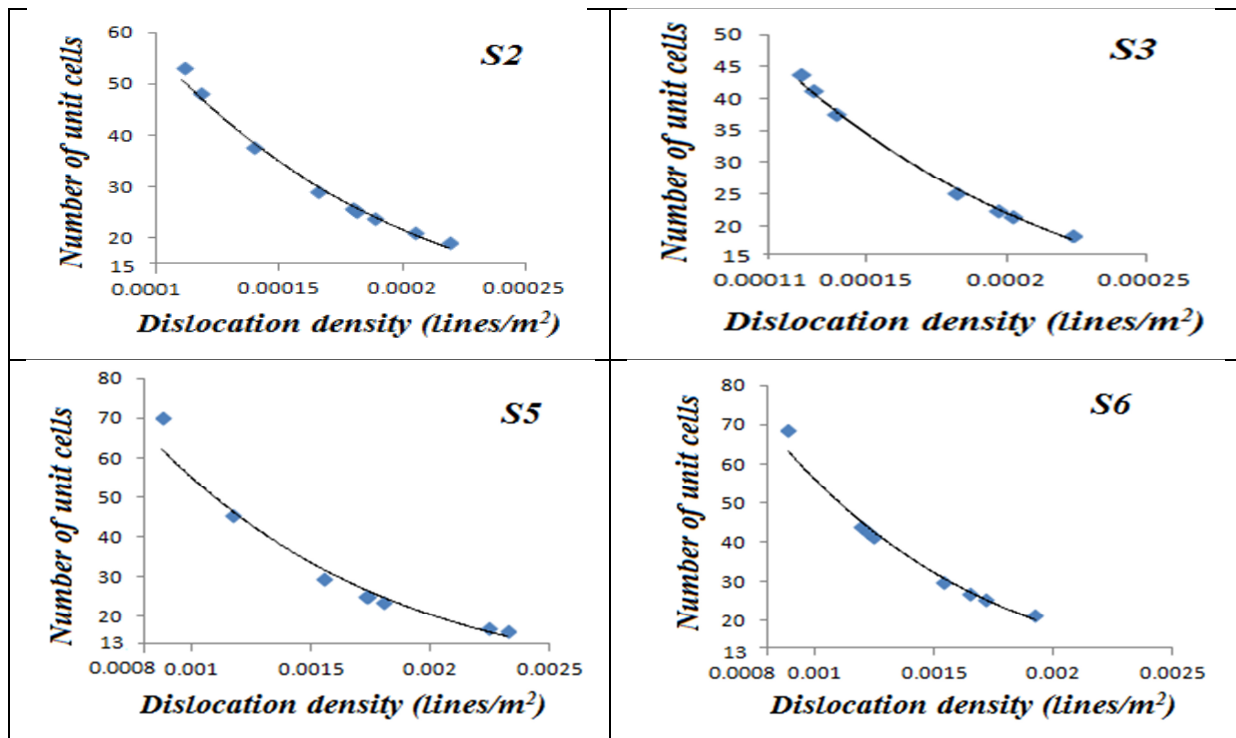
Figure 4. Number of unit cell versus dislocation density of Cr_2O_3-NPs
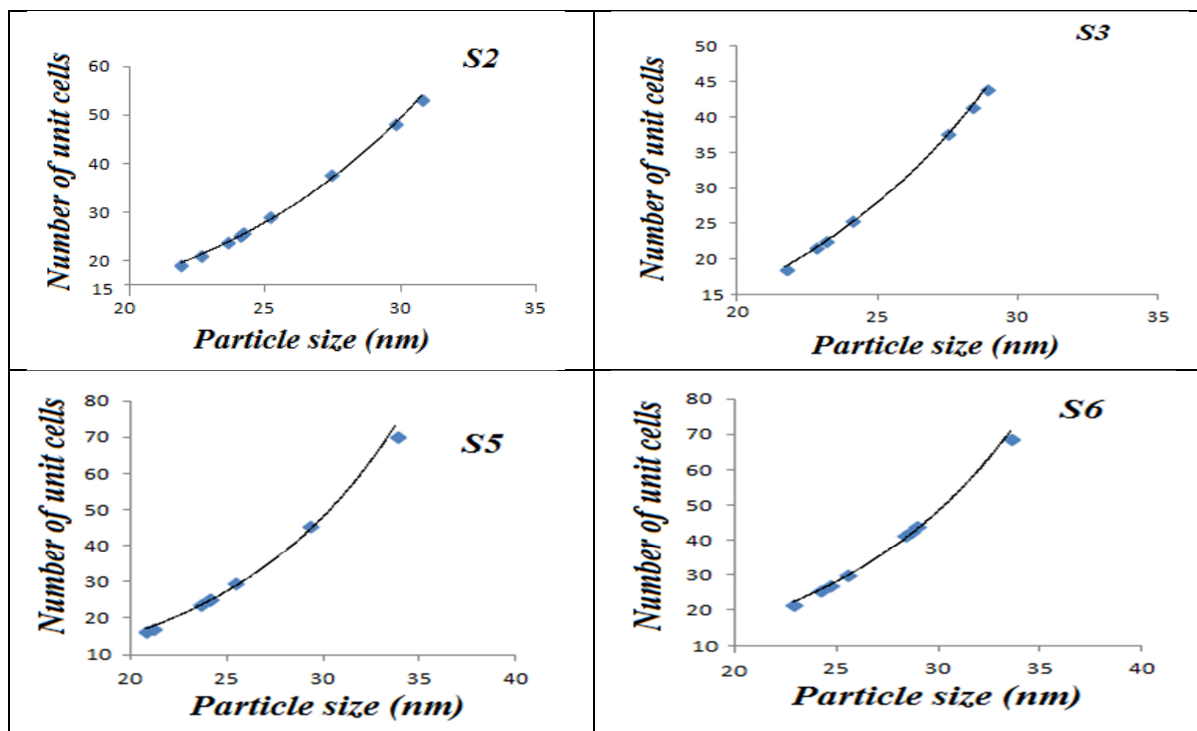
Figure 5. Number of unit cell versus particle size of Cr_2O_3-NPs

3-6 Fourier Transform Infrared Spectroscopy Analysis

Figure (6) shows the typical FTIR spectra of Cr_2O_3-NPs . The spectra represents five sharp absorption bands at 424 cm^{-1}, 487 cm^{-1}, 547 cm^{-1} , 607 cm^{-1} and 638 cm^{-1} respectively. All the observed peaks are in well agreement with the reported results. In general, the metal oxide symbolizes the peaks below 1000 cm^{-1} as a result of inter-atomic vibrations. In the present investigation , the observed peaks illustrate the characteristic peaks of Cr–O bond stretching vibration . As the spectrum reveals the corresponding vibration bands of Cr–O only which in turn depicts the successful removal of impurity contents during calcinations and the high purity of the as-grown Cr_2O_3-NPs. High intensity of the peaks of Cr_2O_3 bands indicates the good crystalline nature of the materials [3].
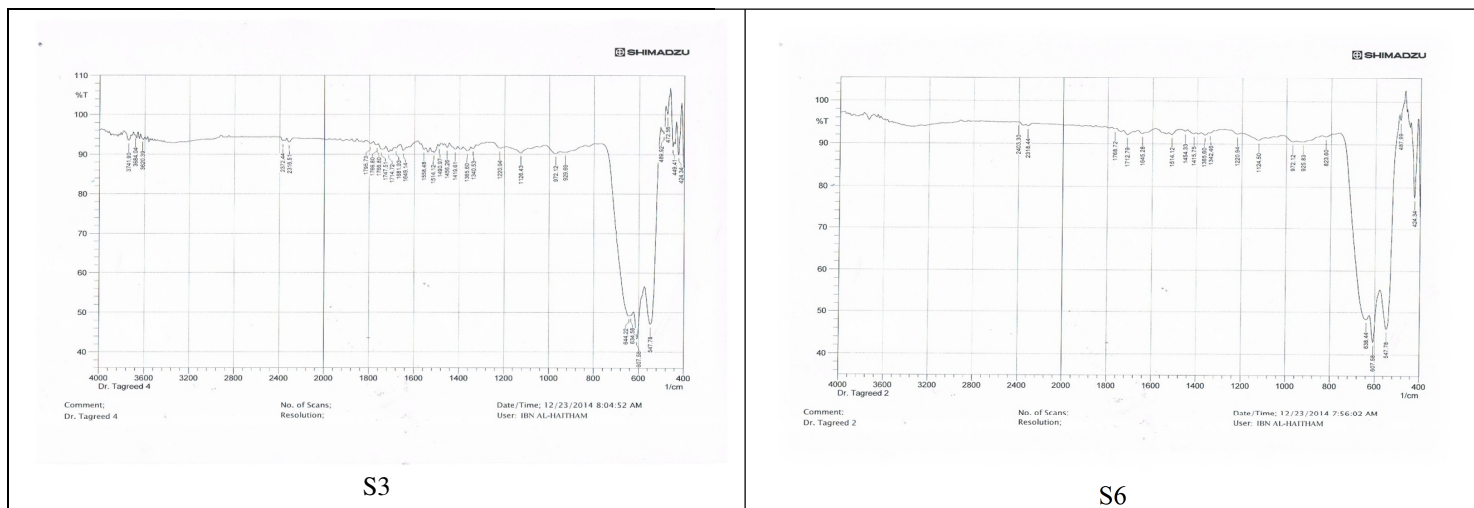
Figure 6. FTIR spectra of Cr_2O_3-NPs

3-7 SEM images analysis

The SEM micrographs for Cr_2O_3-NPs S3 and S6 are shown in figure (7), this Figure shows all particles exhibit a spherical shape with a high degree of agglomeration among fine particles. Figure (7b) shows the increase concentration of (TEA) , the average crystallite size increase and more agglomeration occurs among particles.
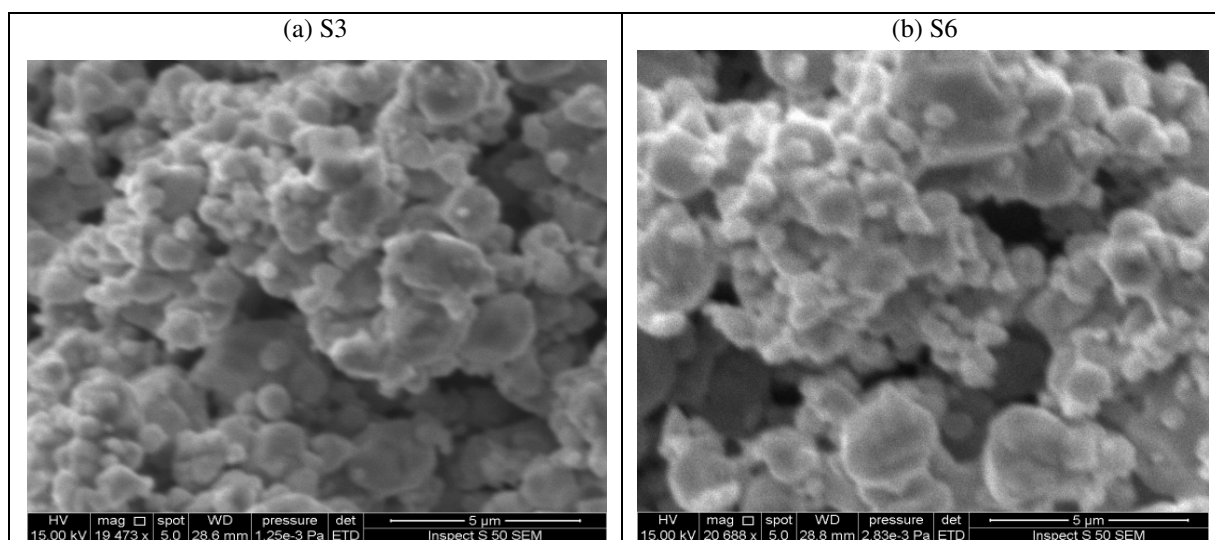
Figure 7. SEM images of Cr_2O_3-NPs

4- Conclusions

Chromium oxide nanoparticles (Cr_2O_3-NPs) with a rhombohedral structure have been prepared successfully by sol-gel method using $Cr(NO_3)3.9H_2O$ as precursor material, triethanolamine (TEA) as template and water as green solvent under microwave irradiation. The results show that the average crystallite size are estimated by D-S formula and W-H formula of (Cr_2O_3-NPs) for all samples in nanoscale. The average crystallite size increase with the increase of annealing temperature and concentration of (TEA). The crystal lattice distortion ratio $<\varepsilon2>^{1/2}$ and the specific surface area (SSA) are inversely proportional, dislocation density (δ) and the number of unit cells (n) are indirectly proportional to particle size. The obtained results have a good optimization between the observed X-ray diffraction patterns and that are calculated by Rietveld analysis. FTIR spectra validated the purity of Cr_2O_3-NPs. The SEM micrographs of Cr_2O_3-NPs for S3 and S6 show all particles exhibit a spherical shape with a high degree of agglomeration among fine particles.

References

[1] Rakesh, S. Ananda and N. Gowda,(2013), "Synthesis of chromium(III) oxide nanoparticles by electrochemical method and mukia maderaspatana plant extract, characterization, $KMnO_4$ decomposition and antibacterial study", Modern Research in Catalysis, 2, 127-135. http://dx.doi.org/10.4236/mrc.2013.24018

[2] I. Esparza, M. Paredes, R. Martinez, A. Couto, G. Loredo, L.Velez and O. Dominguez,(2011) , "Solid stae reactions in Cr_2O_3-ZnO nanoparticles synthesized by triethanolamine chemical precipitation", Materials Sciences and Applications, 2, 1584-1592. doi:10.4236/msa.2011.211212 Published Online November 2011

[3] M. Abdullah, F. Rajab and S. Al-Abbas, (2014) ,"Structural and optical characterization of Cr_2O_3 nanostructures: Evaluation of its dielectric properties", AIP Advances, 4, 027121,1-11. http://dx.doi.org/10.1063/1.4867012

[4] X. Yang, X. Peng, C. Xu, and F. Wang,(2009) , "Electrochemical assembly of Ni – xCr – yAl nanocomposites with excellent high-temperature oxidation resistance", Journal of Electrochemical Society, 156, 167-175. doi: 10.1149/1.3082378

[5] C. Ramesh, K. kumar, M. Senthil and V. Ragunathan , (2012) , "Antibacterial activity of Cr_2O_3 nanoparticles against E.coli; reduction of chromate ions by arachis hypogaea leaves", Archives of Applied Science Research, 4, 1894-1900. (http://scholarsresearchlibrary.com/archive.html)

[6] X. Hou and K. L. Choy,(2008), "Synthesis of Cr_2O_3-based nanocomposite coating within corporation of inorganic fullerene-like nanoparticles", Thin Solid Films , 23, 8620-8624. http://jsciences.ut.ac.ir

[7] X. Pang, K. Gao, F. Luo, Y. Emirov, A. Levin and A. Volinsky,(2009) , "Investigation of micro structure and mechanical properties of multi-layer Cr/Cr_2O_3 coatings,", Thin Solid Films, 6, 1922-1927. doi:10.1016/j.tsf.2008.10.026.

[8] L. Alrehaily, J. Joseph, A. Musa, D. Guzonas and J. Wren, (2013) ," Gamma-radiation induced formation of chromium oxide nanoparticles from dissolved dichromate", Physical Chemistry Chemical Physics, 15, 98-107. doi: 10.1039/c2cp43150e.

[9] V. Jaswal, A. Arora, M. Kinger, V. Gupta and J. Singh,(2014) , "Synthesis and characterization of chromium oxide nanoparticles", Oriental Journal of Chemistry, 30, 559-566. doi : http://dx.doi.org/10.13005/ojc/300220.

[10] S. El-Sheikh, R. Mohamed and O. Fouad, (2009) "Synthesis and structure screening of nanostructured chromium oxide powders", Journal of Alloys and Compounds, 482, 302-307. doi:10.1016/j.jallcom.2009.04.011.

[11] J. Mougin, T. Le Bihan, G. Lucazeau, (2001) "High-pressure study of Cr_2O_3 obtained by high-temperature oxidation by X-ray diffraction and Raman spectroscopy", Journal of Physics and Chemistry of Solids, 62, 553-563. doi:10.1016/S0022-3697(00)00215-8

[12] Z. Pei, H. Xu and Y. Zhang, (2009) " Preparation of Cr_2O_3 nanoparticles via C_2H_5OH hydrothermal reduction", Journal of Alloys and Compounds, 468, 5-8. doi:10.1016/j.jallcom.2007.12.086

[13] U. Balchandran, R. Siegel, Y. Liao and T. As- kew,(1995), "Synthesis, sintering and magnetic properties of nanophase Cr_2O_3", Nanostructure. Mater, 5, 505-512. doi:10.1016/0965-9773(95)00266-H

[14] VD Mote, Y. Purushotham and BN Dole, (2012) , "Williamson-Hall analysis in estimation of lattice strain in nanometer-sized ZnO particles", Journal of Theoretical and Applied Physics, 6, 1–8. http://www.jtaphys.com/content/2251-7235/6/1/6.

[15] A. K. Zak, W.H. Abd. Majid , M.E. Abrishami and R. Yousefi, (2011) ,"X-ray analysis of ZnO nanoparticles by Williamson-Hall and size-strain plot methods", Solid State Sciences, 13, 251–256. doi:10.1016/j.solidstatesciences.2010.11.024.

[16] B. R Rehani, P B Joshi, K. N Lad and A. Pratap, "Crystallite size estimation of elemental and composite silver nano-powders using XRD principles", (2006) ," Indian Journal of Pure & Applied Physics, 4, 157–161. www.researchgate.net/.../266091547.

[17] Y. T. Prabhu, K. V. Rao, V. S. Sai Kumar and B. S. Kumari, (2013) ,"X-ray analysis of Fe doped ZnO nanoparticles by Williamson-Hall and size-strain plot", International Journal of Engineering and Advanced Technology (IJEAT), 4, 268-274. www.ijeat.org/attachments/File/v2i4/D1393042413.

[18] R. E. Goforth, K. T. Hartwig and L. R. Cornwell (auth.), T. C. Lowe, R. Z. Valiev (eds.),((2000) "Investigations and applications of severe plastic deformation", Springer-science and Business media dordrecht,. doi:10.1007/978-94-011-4062-1 .

[19] F. Atallah, (2013) ," The effect of thermal annealing on the structural and optical properties of CdS thin films deposited by vacuum evaporation method", J. of university of Anbar for pure science, 7. www.iasj.net/iasj?func=fulltext&aId=84584.

[20] H. Ahmed and A. Dakhel , (2012) , "The effect of the solution concentration on structural and optical properties CdS thin films prepared by chemical bath deposition technique", International Journal of Recent Research and Review, 5. www.ijrrr.com/papers4/paper2

[21] A. K. Zak, W. H. A. Majid, M. E. Abrishami and R. Yousefi,(2011) ,"X-ray analysis of ZnO nanoparticles by Williamson-Hall and size-strain plot methods", Solid State Sciences, 13, 251-256.

[22] M. E. Nielsen and M. R. Fisk, (2008), Data report: specific surface area and physical properties of subsurface basalt samples from the east flank of Juan de Fuca Ridge, Proceedings of the Integrated Ocean Drilling Program, 301. http://dx.doi.org/10.4236/wjnse.2014.41004

[23] A. Rahdar ,V. Arbabi , and H.Ghanbari, (2012) , "Study of electro - optical properties of ZnS nanoparticles prepared by colloidal particles method " , Int. J. of Chemical and Biological Engineering , 6.

[24] T. Theivasanthi and M. Alagar,(2013) , "Konjac biomolecules assisted–rod/ spherical shaped lead nano powder synthesized by electrolytic process and its characterization studies", Nano Biomed. Eng. 5, 11-19.doi : 10.5101/nbe.v5i1.p11-19.

[25] T. Theivasanthi and M. Alagar, (2012) ,"Electrolytic synthesis and characterization
of silver nanopowder", Nano Biomed. Eng. 4, 58-65.doi : 10.5101/nbe.v4i2.p58-65

[26] A. Gaber, M. Abdel- Rahim, A. Abdel-Latief and M. Abdel-Salam , (2014) ,"
 Influence of Calcination Temperature on the Structure and Porosity of Nanocrystalline SnO_2 Synthesized by a Conventional Precipitation method ", Int. J. Electrochem. Sci., 9, 81-95. www.electrochemsci.org

[27] H.M. Rietveld, (1969) ,"Profile refinement method for nuclear and magnetic structures", J. Appl. Cryst., 2, 65–71. doi:10.1107/S0021889869006558

[28] R. A. Young , (1995) , "The Rietveld method" , Oxford University Press INc., New York .

[29] H. M. Rietveld, (1967) , "Line profiles of neutron powder-diffraction peaks for structure refinement", Acta Cryst., 22, 151–152. doi:10.1107/S0365110X67000234

[30] K. Kapoor, D. Lahiri, S. V. R. Rao, T. Sanyal and B. P. Kashyap, (2004) , "X-ray diffraction line profile analysis for defect study in Zr–2×5% Nb material", Bull. Mater. Sci., 27, 59–67. www.ias.ac.in/matersci/bmsfeb2004/59

[31] I. C. Dragomir, D. S. Lia, G. A. Castello-Branco, H. Garmestani, R. L. Snyder, G. Ribarik and T. Ungar,(2005) , " Evolution of dislocation density and character in hot rolled titanium determined by X-ray Influence of calcination temperature on the structure and porosity of nanocrystalline SnO_2 synthesized by a conventional precipitation method diffraction", Materials Characterization, 55, 66–74.

[32] T. Shintani, Y. Murata, Y. Terada and M. Morinaga , (2010) ,"Evaluation of dislocation density in a Mg-Al-Mn-Ca alloy determined by X-ray diffractometry and transmission electron microscopy", Materials Transactions, 51, 1067–1071. doi:10.2320/matertrans.M2010021

[33] M. A. M. Khan, S. Kumar, M. Ahamed, S. A. Alrokayan and M. S. AlSalhi, "Structural and thermal studies of silver nanoparticles and electrical transport study of their thin films", Nanoscale Research Letters, 2011, 6. doi: 10.1186/1556-276X-6-434

[34] N. Q. Chinh, J. Gubicza and T. G. Langdon, "Characteristics of face-centered cubic metals processed by equal-channel angular pressing", J. Mater. Sci., 42 (2007), pp. 1594–1605. doi:10.1007/s10853-006-0900-3

The IISTE is a pioneer in the Open-Access hosting service and academic event management. The aim of the firm is Accelerating Global Knowledge Sharing.

More information about the firm can be found on the homepage:
http://www.iiste.org

CALL FOR JOURNAL PAPERS

There are more than 30 peer-reviewed academic journals hosted under the hosting platform.

Prospective authors of journals can find the submission instruction on the following page: http://www.iiste.org/journals/   All the journals articles are available online to the readers all over the world without financial, legal, or technical barriers other than those inseparable from gaining access to the internet itself.   Paper version of the journals is also available upon request of readers and authors.

MORE RESOURCES

Book publication information: http://www.iiste.org/book/

Academic conference: http://www.iiste.org/conference/upcoming-conferences-call-for-paper/

IISTE Knowledge Sharing Partners

EBSCO, Index Copernicus, Ulrich's Periodicals Directory, JournalTOCS, PKP Open Archives Harvester, Bielefeld Academic Search Engine, Elektronische Zeitschriftenbibliothek EZB, Open J-Gate, OCLC WorldCat, Universe Digtial Library , NewJour, Google Scholar